



Published in final edited form as:

Anal Chem. 2006 July 15; 78(14): 4839–4849.

On-Chip Titration of an Anticoagulant Argatroban and Determination of the Clotting Time within Whole Blood or Plasma Using a Plug-Based Microfluidic System

Helen Song[†], Hung-Wing Li[†], Matthew S. Munson[†], Thuong G. Van Ha[‡], and Rustem F. Ismagilov^{*,†}

Department of Chemistry and Institute for Biophysical Dynamics, University of Chicago, 5735 South Ellis Avenue, Chicago, Illinois 60637, and Department of Radiology, Section of Interventional Radiology, University of Chicago, 5841 South Maryland Avenue, MC 2026, Chicago, Illinois 60637

Abstract

This paper describes extending plug-based microfluidics to handling complex biological fluids such as blood, solving the problem of injecting additional reagents into plugs, and applying this system to measuring of clotting time in small volumes of whole blood and plasma. Plugs are droplets transported through microchannels by fluorocarbon fluids. A plug-based microfluidic system was developed to titrate an anticoagulant (argatroban) into blood samples and to measure the clotting time using the activated partial thromboplastin time (APTT) test. To carry out these experiments, the following techniques were developed for a plug-based system: (i) using Teflon AF coating on the microchannel wall to enable formation of plugs containing blood and transport of the solid fibrin clots within plugs, (ii) using a hydrophilic glass capillary to enable reliable merging of a reagent from an aqueous stream into plugs, (iii) using bright-field microscopy to detect the formation of a fibrin clot within plugs and using fluorescent microscopy to detect the production of thrombin using a fluorogenic substrate, and (iv) titration of argatroban (0–1.5 $\mu\text{g}/\text{mL}$) into plugs and measurement of the resulting APTTs at room temperature (23 °C) and physiological temperature (37 °C). APTT measurements were conducted with normal pooled plasma (platelet-poor plasma) and with donor's blood samples (both whole blood and platelet-rich plasma). APTT values and APTT ratios measured by the plug-based microfluidic device were compared to the results from a clinical laboratory at 37 °C. APTT obtained from the on-chip assay were about double those from the clinical laboratory but the APTT ratios from these two methods agreed well with each other.

This paper describes the development of a plug-based microfluidic system capable of titrating an anticoagulant drug, argatroban, into human blood samples and measuring the resulting clotting times. A method for injecting reagents into flowing plugs is also described. Determining the correct dose of an anticoagulant drug is important, as too little of the drug will not be effective while too much of the drug can result in uncontrolled bleeding. Argatroban directly inhibits the active site of thrombin, an essential enzyme in the coagulation cascade.¹ This inhibitor is an effective treatment for heparin-induced thrombocytopenia (HIT).² Heparin is a common anticoagulant used to treat thromboembolic diseases and to prevent thrombosis

* To whom correspondence should be addressed. E-mail: r-ismagilov@uchicago.edu..

[†]Department of Chemistry and Institute for Biophysical Dynamics.

[‡]Department of Radiology.

SUPPORTING INFORMATION AVAILABLE

Additional information as noted in the text: a movie of the merging junction with the hydrophilic glass capillary, where CaCl_2 solution is injected into a plug containing whole blood; a movie of a single plug being followed through a microchannel as a fibrin clot formed within the plug; and characterization of the size of the aqueous plug and the carrier fluid spacing between plugs for various water fractions. This material is available free of charge via the Internet at <http://pubs.acs.org>.

in vascular procedures and after certain surgeries. However, with prolonged use of heparin, ~50% of patients develop antibodies to heparin³ and ~5% develop HIT,¹ a heparin-induced immune response that results in an uncontrolled hypercoagulable state, which can lead to deep vein thrombosis, multiple organ failure, amputation, and even death. In medical procedures, argatroban can be used as heparin substitute in patients in whom heparin use is contraindicated.

Currently, the appropriate dose of argatroban is determined for each patient individually. First, the baseline clotting time is measured of the patient's blood sample. Then, a protocol is followed where a certain amount of argatroban is administered intravenously, a blood sample is drawn after 2 h (the steady-state levels of drug and anticoagulant activity are reached within 1–3 h), and the clotting time is measured.⁴ This clotting time is determined using the activated partial thromboplastin time (APTT) test, which typically takes another 1–2 h for a central clinical laboratory to process.⁵ After this test, the administered dose of argatroban is adjusted accordingly and this protocol is repeated until the clotting time is 1.5–3.0 times the baseline clotting time. The entire process of determining the correct dose of the anticoagulant may take half a day while causing significant patient discomfort from multiple needle sticks to obtain blood samples. Therefore, an appropriate dose for a patient can be determined more efficiently and conveniently if there is a rapid and reliable in vitro assay that performs these titrations using a minimal amount of the patient's blood prior to argatroban administration. Ideally, the dose is predetermined and aPTT is measured at most once at steady state for confirmation after administration.

Microfluidic systems have been applied for a range of biological assays^{6–11} that benefit from aspects of miniaturization, such as smaller sample requirement, shorter analysis time, and higher levels of automation and high-throughput. These lab-on-a-chip technologies have been implemented with blood samples¹² for rapid analyte detection,^{13–16} on-chip cell separation,^{16–20} micro-thrombus formation,²¹ platelet activation,²² plasma separation from whole blood,²³ blood rheology,^{24,25} and red blood cell analysis.^{26–29} In addition, commercially available point-of-care devices have been developed, where a droplet of blood (~15–50 μL) is drawn into a microcapillary by capillary action and formation of the clot is detected by various mechanical and optical methods.^{5, 30–37} There are various methods for detection of the fibrin clot within these devices, such as the use of magnetic particles, LED optical detectors, a plunger assembly, an amperometer, a laser beam to detect transmittance, or an ultrasonic probe.³² A wide range of point-of-care devices are commercially available and have been used when rapid turnaround time (minutes versus ~1–2 h for results from a central clinical laboratory) is essential, such as for cardiac surgery.^{5,32} Results from these point-of-care devices and from clinical laboratories have been determined to be comparable,^{33–35} and devices are even available for home use.^{30,36}

There are four difficulties when using single-phase flow in microfluidics to titrate drugs into blood samples while measuring the resulting clotting times. First, pressure-driven laminar flow results in dispersion of reagents along the channel. Second, laminar flow also results in slow mixing. Third, due to the high surface area-to-volume ratio in microfluidic devices, surface adsorption must be controlled to ensure correct analysis. Fourth, the formation of aggregates and clots may result in contamination or blockage of the microchannels. Commercially available micro-capillary devices use single-phase flow and are for single use only. However, the titration of reagents using single-phase flow can be achieved by using multichannel devices where each channel contains a different concentration of the reagent.

Multiphase flow in microfluidics systems can address the problems that arise in single-phase flow. By forming air–liquid segments within capillaries,^{38–41} segmented flow injection analysis has been used for automated analysis of samples, including blood.^{42,43} Discrete air bubbles were used to separate aqueous samples within the capillaries.

We emphasize that plug-based microfluidics (liquid–liquid segmented flow) differs fundamentally from air–liquid segmented flows. In air–liquid segmented flow, dispersion is reduced with the use of air bubbles (compared to flow without bubbles) but it is not eliminated. Also, the aqueous sample is in direct contact with the capillary, which results in cross-contamination of samples. Therefore, the surface chemistry of the capillary must be treated to inhibit adsorption of the fibrin clot. On the scale of nanoliter volumes, surface chemistry becomes especially important, and generally, there are two solutions to address this problem. The surface can be treated to inhibit any adsorption of the sample, or droplets can be used to encapsulate the sample so that the sample is not in contact with the surface. In a plug-based microfluidic system, flows of immiscible aqueous and fluoruous liquids are used to form plugs (nanoliter-sized droplets) within the microchannels and result in four differences between air–liquid versus liquid–liquid segmented flows. First, dispersion is eliminated by encapsulating the aqueous reagents within the plugs, and cross-contamination between plugs is also eliminated.^{44,45} Second, the products from the reaction do not adsorb to and contaminate the walls of the microchannel. The reaction occurs within the dispersed phase (aqueous) and only the continuous phase (fluoruous) is in contact with the surface of the microchannel. Therefore, the products of the reaction remain contained within the plugs, including even solid products that otherwise would adhere to the walls.⁴⁶ Third, mixing within plugs can be very rapid by using chaotic advection induced by winding channels.^{45, 47–49} These winding channel designs have also been incorporated for air–liquid segmented flow systems to achieve rapid mixing.⁵⁰ Fourth, the surface chemistry at the aqueous–fluoruous interface of plugs can be controlled using fluoruous-soluble surfactants that do not appear to interfere with the proteins in the aqueous phase.⁵¹ Plug-based systems can perform the same functions as air–liquid segmented flow systems, but plugs also maintain the four advantages that was described above. Plug-based microfluidic systems provide chemical microreactors with well-controlled mixing,^{47,52} biocompatibility at the aqueous–fluoruous interface,⁵¹ capability of titrating reagents,^{53,54} and merging of reagents.^{45,46,55} Under a steady flow of plugs traveling through the microchannel, each position along the microchannel corresponds to a specific residence time.^{45,47,54} One can also follow a reaction over time by following plugs moving along the microchannel.

Droplet-based microfluidic systems relying on liquid–liquid segmented flow have been developed^{45,56–65} and used for applications such as PCR amplification,^{66,67} measurement of enzyme kinetics,^{51,54} cell and protein encapsulation,^{68–70} growth of cell cultures,^{71,72} and formation of particles.^{46,52,73–77} Droplet-based microfluidic systems relying on gas–liquid segmented flow have also been developed^{50,78} and used for analyte detection⁷⁹ and DNA analysis.⁸⁰ Electrowetting has been used for dispensing, transporting, and mixing within droplets^{81–84} and has been used for applications such as droplet formation containing various human fluids,⁸⁵ glucose detection,⁸⁶ peptide analysis using mass spectrometry,^{87,88} and synthesis of polymer particles.⁸⁹

In this paper, we determined the APTT using a plug-based microfluidic platform with and without titrating argatroban. When coagulation is initiated via the intrinsic pathway, the APTT is the elapsed time between the addition of CaCl_2 and the detection of a fibrin clot in the blood sample.¹ To measure the APTT on-chip, we further developed the plug-based microfluidic technology to achieve the following: (i) form plugs containing blood and transport the solid clots within the plugs through microchannels without contaminating the walls; (ii) control the merging of a reagent into a plug, which is important for multistep assays such as the APTT test; (iii) detect clots within plugs containing whole blood or plasma; and (iv) titrate argatroban into plugs and measure the resulting APTTs at 23 and 37 °C.

EXPERIMENTAL SECTION

Reagents and Solutions

All aqueous solutions were prepared in 18-M Ω deionized water (Millipore, Billerica, MA). All reagents were purchased from Sigma-Aldrich (St. Louis, MO) unless otherwise specified. A fluorogenic substrate for human α -thrombin, *tert*-butyloxycarbonyl- β -benzyl-L-aspartyl-L-prolyl-L-arginine-4-methyl-coumaryl-7-amide ($\lambda_{\text{ex}} = 365$ nm, $\lambda_{\text{em}} = 440$ nm), was purchased from Peptide Institute, Inc. (Osaka, Japan). For this substrate, kinetic parameters at 37 °C were $k_{\text{cat}} = 160$ s $^{-1}$, $K_{\text{M}} = 11$ μ M in buffer solution of 50 mM Tris-HCl, pH 8.0, with 0.15 M NaCl, 1 mM CaCl₂, and 1 mg/mL BSA.⁹⁰ The APTT reagent, Sigma Diagnostics Alexin, was obtained from Trinity Biotech (Wicklow, Ireland). Argatroban (stock concentration of 100 mg/mL) was obtained from GlaxoSmithKline (Philadelphia, PA). This stock was diluted to 1 mg/mL with 150 mM NaCl, 20 mM Tris, pH 7.8, prior to the experiment. 1*H*,1*H*,2*H*,2*H*-perfluoro-1-octanol (PFO, 98%) was obtained from Alfa Aesar.

Protocol for the APTT Assay

(a) Collection of Blood Samples—Blood samples were obtained from healthy donors with approval from Institutional Review Board (protocol 12502A) by the Department of Radiology at the University of Chicago Hospitals. Whole blood was collected in Vacutainer tubes at a ratio of 1 part 3.2% sodium citrate to 9 parts blood to obtain decalcified whole blood. Tubes were gently shaken to mix the contents. For experiments using donor's whole blood (which contains both cells and plasma), samples were used from the Vacutainer tubes without further processing. For experiments using donor's platelet-rich plasma (PRP), plasma was obtained after the samples from Vacutainer tubes were centrifuged twice at 1600 rpm for 10 min.⁹¹ Normal pooled plasma (platelet-poor plasma, PPP) was obtained from George King Biomedical (Overland Park, KS) and stored at -80 °C. These pooled plasma samples were composed of plasma from at least 30 healthy donors. For experiments using normal pooled plasma (PPP), samples were defrosted and then centrifuged at 1500 rcf for 15 min to remove the deposited debris resulted from prolonged storage.

(b) Typical Procedure for Measuring the APTT—The reaction network of blood coagulation is composed of ~80 biochemical reactions among many proteins, including those called clotting factors.¹ These reactions are generally categorized into two pathways: the intrinsic pathway and the extrinsic pathway. The APTT assay measures the time required for clotting when initiated by the intrinsic pathway. APTT reagents contain two components: (i) negatively charged particles that bind factor XII to initiate the intrinsic pathway and (ii) phospholipids to provide binding sites required for factor complexes. For Alexin, the APTT reagent used in this work, the activator was ellagic acid and the phospholipid was rabbit brain cephalin. First, one part of decalcified blood samples is mixed with one part of Alexin and the resultant mixture is incubated for 3 min to sufficiently activate the intrinsic pathway of coagulation. This mixture of plasma and Alexin is then recalcified with one part of 20–25 mM CaCl₂.⁴ The final concentration of CaCl₂ is ~7–8 mM. Excess CaCl₂ is used to overcome the effect of citrate. Finally, the time that elapses between the addition of CaCl₂ and the detection of fibrin clots within the sample is recorded as the APTT. This procedure was used as a guideline for adapting the plug-based microfluidic device to measure the APTT.

Clinical results for the APTTs were measured with the STA Coagulation Analyzer (Diagnostica Stago, Inc., Parsippany, NJ) by the Coagulation laboratory at the University of Chicago Hospital.

Microfluidic Setup

(a) Fabrication of Devices—Microfluidic devices were fabricated using rapid prototyping in poly(dimethylsiloxane) (PDMS).^{9,92,93} Microchannels were rendered hydrophobic and fluorophilic using the silanization protocol described previously⁵¹ with the exception that tridecafluoro-1,1,2,2,-tetrahydrooctyl)-1-trichlorosilane vapor flowed into the device for 1.5 h rather than 1 h. In addition to the silanization protocol, the microchannels were coated with amorphous Teflon (Teflon AF 1600, poly[4,5-difluoro-2,2-bis(trifluoromethyl)-1,3-dioxole-co-tetra-fluoroethylene]).^{94–96} First, microchannels were filled with a 1% (w/v) Teflon AF 1600 solution in a 1:4 (v/v) mixture of FC-70 and FC-3283. For experiments conducted at 37 °C, microchannels were filled with a 2.5% (w/v) Teflon AF 1600 solution in a 1:1 (v/v) mixture of FC-70 and FC-3283. Then, devices were baked at 70 °C overnight until the solution evaporated. Composite glass/PDMS capillary devices were fabricated as described previously⁹⁷ with the exception that glass capillaries were rendered hydrophilic using a Plasma Prep II plasma cleaner before coupling to the PDMS device.

(b) Microfluidic Experiments—Microfluidic experiments were conducted as described previously^{51,54,65} with the following modifications. Plugs were formed using a fluorinated carrier fluid, which was a mixture of 10:1 (v/v) FC-70/PFO, where $\gamma = 10 \text{ mN m}^{-1}$ and $\mu = 24 \text{ mPa s}$ at 23 °C. Harvard Apparatus PHD 2000 infusion pumps were used to drive flows within devices. Flow rate of the fluorinated carrier fluid was maintained at 3 $\mu\text{L}/\text{min}$. Aqueous solutions used to form plugs were Alexin and blood samples (which were either whole blood, platelet-rich plasma, or platelet-poor plasma; more information in the next paragraphs). For Alexin, the flow rate was 0.3 $\mu\text{L}/\text{min}$ for experiments conducted at 23 °C and 1.2 $\mu\text{L}/\text{min}$ for experiments conducted at 37 °C. For the two blood streams, the total flow rate was 0.3 $\mu\text{L}/\text{min}$ for 23 °C and 1.2 $\mu\text{L}/\text{min}$ for 37 °C. A droplet of 100 mM CaCl_2 solution (300 mOs) was injected into each plug at the merging junction. The flow rate of the CaCl_2 solution was 0.2 $\mu\text{L}/\text{min}$ for 23 °C and 0.4 $\mu\text{L}/\text{min}$ for 37 °C. Estimated from the flow rate of the Alexin, the two blood streams and the CaCl_2 solution, the concentration of CaCl_2 was 25 and 14 mM for experiments at 23 and 37 °C, respectively. Excess CaCl_2 was used to overcome the effect of citrate. For experiments at 37 °C, a microscopic heating stage (Brook Industries, Lake Villa, IL) was used to keep the devices at 37 °C.

In all figures (except in Figure 2), the main PDMS channel of the microfluidic device was 300 $\mu\text{m} \times 270 \mu\text{m}$ (width \times height), and the small channel was 100 $\mu\text{m} \times 100 \mu\text{m}$. In Figure 2a, the main PDMS channel and the side channel both were 200 $\mu\text{m} \times 250 \mu\text{m}$. In Figure 2b, the main PDMS channel was 200 $\mu\text{m} \times 250 \mu\text{m}$, and the small side channel was 50 $\mu\text{m} \times 50 \mu\text{m}$. In Figure 2c, the main PDMS channel was 200 $\mu\text{m} \times 260 \mu\text{m}$, and the height of the sidearm and the corner volume was 80 μm .

(c) Measurement of the APTT with Whole Blood Samples—For microfluidic experiments with whole blood, the stock solutions in the aqueous syringes were (i) Alexin, (ii) whole blood, and (iii) whole blood with 3.0 $\mu\text{g}/\text{mL}$ argatroban. Experiments were conducted using either a Leica DM IRB or DMI6000 microscope. Fibrin clots within plugs formed with whole blood were detected optically using a Spot Insight color digital camera (Diagnostics Instruments, Inc).

(d) Measurement of the APTT with Plasma Samples—For microfluidic experiments with plasma (either platelet-rich or platelet-poor), the stock solutions in the three aqueous syringes were (i) Alexin, (ii) plasma with 140 μM fluorogenic substrate, prepared by adding 3.5 μL of the stock substrate solution (10 mM in DMSO) into 246.5 μL of plasma, and (iii) plasma with 140 μM fluorogenic substrate and 3.0 $\mu\text{g}/\text{mL}$ argatroban, prepared by adding 3.5 μL of the stock substrate solution and 0.75 μL of argatroban (1 mg/mL) into 245.5 μL of plasma.

Experiments were conducted using a Leica DMI6000 microscope. Cleavage of the fluorogenic substrate for α -thrombin was monitored on the microscope by fluorescence, using a DAPI filter ($\lambda_{\text{ex}} = 350 \pm 25$ nm, $\lambda_{\text{em}} = 460 \pm 25$ nm) and a cooled CCD ORCA ERG 1394 (12-bit, 1344 \times 1024 resolution) (Hamamatsu Photonics, K. K., Hamamatsu City, Japan). Fibrin clots within plasma samples was monitored on the microscope by bright-field microscopy.

RESULTS AND DISCUSSION

Overall Design of the Microfluidic Chip for Performing the APTT Test

The microfluidic device consisted of five different regions: the plug-forming region, the mixer, the incubation region, the merging junction, and the detection region (Figure 1). Plugs of the three aqueous reagents were formed: (i) Alexin, (ii) decalcified blood, and (iii) decalcified blood mixed with argatroban. The blood sample was either donor's whole blood, donor's PRP or PPP. The flow rate of the Alexin and the combined flow rate of the blood streams were maintained at a 1:1 ratio, as required by the APTT assay (see Experimental Section for more information). By varying the relative flow rates of the two blood streams, the concentration of argatroban within plugs was varied.^{53,54} Winding channels were incorporated into the design of the microfluidic network to promote mixing of the reagents within plugs.^{47,52} The length of microchannel in the incubation region was specifically designed so that, at the total flow rate of the aqueous and fluorinated carrier fluid streams, the incubation time of the plugs was 3 min, as specified by the APTT assay (Figure 1, upper region of microchannel network).

The merging junction was required to inject CaCl_2 into the plug after incubation (Figure 1, right side of microchannel network, indicated in blue). More information about this junction is given below. To accelerate mixing of CaCl_2 within the plug, another winding channel was designed into the microchannel network. The starting time of the APTT ($t = 0$) was established when the plugs of blood were merged with the CaCl_2 solution at the merging junction. This is consistent with the one used in clinical laboratories where the starting time of the APTT assay equals the time of addition of CaCl_2 to the blood sample. However, in our preliminary microfluidic experiments, the clotting time appeared to be dependent on the rate of mixing (data not shown). The rate of mixing is known to affect a wide range of autocatalytic systems.⁹⁸ The effect of mixing on the clotting time will be further investigated using a recently developed "bumpy" microfluidic mixer, which accelerated chaotic mixing within plugs of viscous biological samples.⁴⁹ For more reliable transport of the fibrin clots inside the plugs without sticking to the PDMS microchannel wall, the surface of the microchannel was first treated with a fluorinated silane and then coated with amorphous Teflon (see Experimental Section for more information). To determine the time at which fibrin clots formed within the plug, images were taken and analyzed by bright-field and fluorescence microscopy in the detection region (Figure 1, lower region of the microchannel network).

Two New Methods of Merging a Stream into Flowing Plugs

To perform a multistep assay on a plug-based microfluidic system, injection of reagents into a plug is necessary.^{45,46,55,99,100} Three merging methods were previously developed for plug-based microfluidics: (i) the reagent was directly injected into a plug as it moved past the channel containing the reagent;⁴⁶ (ii) a small droplet was merged into an adjacent larger plug in the main channel when the frequency was matched between formation of the droplet and of the plug;⁴⁵ (iii) 10 smaller droplets were merged into a single larger plug.⁵⁵ However, these three methods were difficult to implement in this assay. At these slow flow rates (0.1–0.2 mm/s for the CaCl_2 stream), contamination of the CaCl_2 stream occurred in the side channel when CaCl_2 was directly injected into the passing plug (Figure 2a). If a side junction was used with a smaller width and height, small droplets of CaCl_2 formed and did not merge with the passing plug at the junction (Figure 2b).

Here, we implemented two new approaches for merging. For the first approach, the merging junction was designed so that the fluorinated carrier fluid between the plugs flowed into the sidearm to break off a droplet of CaCl₂ within the corner volume (Figure 2c). To make this design, the size of the aqueous plug and the carrier fluid spacing between plugs was characterized for various water fractions, wf (Supporting Information). Using this design, the frequency was matched between the plug passing that junction and the droplet forming at the corner volume. Successful merging was dependent on the ratio of $U_{\text{CaCl}_2}/U_{\text{aqueous}}$ and not on the water fraction, $wf = U_{\text{aqueous}}/U_{\text{total}}$, where U_{CaCl_2} ($\mu\text{L}/\text{min}$) is the flow rate of the CaCl₂ stream, U_{aqueous} ($\mu\text{L}/\text{min}$) is the total volumetric flow rates of the aqueous streams for blood and Alexin, and U_{total} ($\mu\text{L}/\text{min}$) is the total volumetric flow rates of the blood, Alexin, and carrier fluid streams. Data are included in the Supporting Information to show the dependence of length of plugs and carrier fluid spacing between plugs as a function of wf and U_{total} ($\mu\text{L}/\text{min}$). For wf = 0.4, the highest percentage of successful merging events (95%) was observed when $U_{\text{CaCl}_2}/U_{\text{aqueous}} = 0.125$, where U_{CaCl_2} was maintained at 0.1 $\mu\text{L}/\text{min}$ (Figure 2d, solid symbols). If $U_{\text{CaCl}_2}/U_{\text{aqueous}}$ was maintained at 0.125, then successful merging (92–99%) was observed for various wf from 0.36 to 0.45 (Figure 2d, open symbols). The advantage of this approach was that it did not require extensive fabrication effort. However, merging did not occur consistently over a wide range of $U_{\text{CaCl}_2}/U_{\text{aqueous}}$.

The second approach (Figure 3a) relied on control of surface chemistry of the side channel. We used a small side channel to avoid back-contamination (as in Figure 2b) but made it hydrophilic. The merging junction was fabricated by inserting a hydrophilic capillary into this side channel. The solution of CaCl₂ remained attached to the capillary due to wetting, and the undesirable droplets seen in Figure 2b did not form (movie available in Supporting Information). It is important to (i) insert the capillary flush with the edge of the main channel for this method to work and (ii) have size of blood plugs larger than size of CaCl₂ droplet ($U_{\text{CaCl}_2}/U_{\text{aqueous}} < 1$, typically 0.17–0.33 in experiments here). When these two requirements were satisfied, consistent merging (100%, >40 experiments in different devices) was observed at the flow rates of the aqueous streams (0.6–2.4 $\mu\text{L}/\text{min}$) and the CaCl₂ stream (0.2–0.4 $\mu\text{L}/\text{min}$) we used for APTT assay. The volume of CaCl₂ being injected into the plug, $V_{\text{injected CaCl}_2}$ (nL), linearly increased with the $U_{\text{CaCl}_2}/U_{\text{aqueous}}$ (Figure 3b). Using this method, only small volumes of the CaCl₂ reagent (2–10 nL) could be injected into the plug (~40 nL before merging). By controlling the flow rates, the exact amount of the injecting reagent could be easily controlled. This merging approach was used for direct injection of CaCl₂ solution for APTT measurement for the rest of this paper.

Detecting Clots within Plugs and Analyzing Images To Measure the APTT and Thrombin Generation

The APTT is the elapsed time from the addition of CaCl₂ to the detection of fibrin clots within the blood sample. In most point-of-care devices and commercially available machines used in testing centers, formation of the fibrin clot is detected by detecting changes in optical transmittance or in movement of magnetic particles. In this report, fibrin clots within plugs were detected by bright-field and thrombin generation within plugs was detected by fluorescence microscopy. By analyzing images taken of plugs traveling through the microchannel, we established a standardized method to determine the APTT in plugs.

(a) Detecting Fibrin Clots in Plugs of Donor's Whole Blood—For plugs formed with whole blood, bright-field microscopy was used to detect the trapping of red blood cells (RBCs) within fibrin clots. The APTT was determined to be the time at which the RBCs within the plug were no longer moving (relative to the motion of the plug flowing through the microchannel). Series of images of a single plug were acquired at 2 frames/s (movie available in Supporting Information). To follow a single plug, the microscope stage was moved at the

same speed relative to the speed of the plug moving through the microchannel. Before clotting, the RBCs were evenly distributed and were moved by internal circulation within the plugs.^{45,101} After some time, small clumps of RBCs appeared within the plug but other RBCs still moved by internal circulation (Figure 4a, top image, $t = 121$ s). The shear (~ 2 s⁻¹) within moving plugs was much lower than that required to induce clotting by activating platelets (~ 750 s⁻¹).^{102–104} At a later time, a larger and denser clump of RBCs trapped in a fibrin clot moved to the back half of the plug while the rest of the RBCs did not move due to being trapped within the fibrin network (Figure 4a, bottom image, $t = 136$ s). For the plug shown in Figure 4a, the APTT of the plug was $t = 136$ s at 23 °C. We define t_{trans} (s) as the time that elapses from the first sign of clotting (Figure 4a, top image) to when the RBCs no longer move relative to the plug (Figure 4a, bottom image). For this plug shown in Figure 4a, t_{trans} was 15 s.

The APTT was also determined from many plugs statistically. At each time point, images were acquired for at least 20 plugs. From a set of images at each time point, the number of plugs that contain fibrin clots was counted. This number was divided by the total number of plugs to obtain the “percentage of plugs clotted” at each time point (Figure 4b). The APTT was the time for 50% of plugs of whole blood to be clotted. The APTT was 110 s at 23 °C (Figure 4b), in agreement with previously measured APTTs of 175 ± 58 s at 23 °C and 104 ± 20 s at 25 °C.¹⁰⁵ The average t_{trans} was 15.4 ± 2.8 s for nine plugs of whole blood.

(b) Detecting Clots within Plugs Formed with Donor’s Plasma (Platelet-Rich)—

Clinical laboratories frequently measure the APTT using plasma rather than whole blood. We determined the APTT in plasma with two methods: using bright-field microscopy to observe formation of dense fibrin clots and using fluorescent microscopy to detect cleavage of a fluorogenic substrate by thrombin. To observe fibrin clots in plasma using bright-field microscopy, a time series of images was acquired for a single plug traveling through the microchannel (Figure 5a, left panels). A digital convolution filter Sobel (from Metamorph software) was used to aid the visual detection of the clot (Figure 5a, right panels). For the plug shown in Figure 5a, the APTT was ~ 113 s and t_{trans} was 14 s. We define t_{trans} (s) as the period of time that elapses from the first sign of clotting (Figure 5a, first image) to when the fibrin clot no longer moves relative to the plug (Figure 5a, fifth image).

Using fluorescence microscopy, a more quantitative determination of the thrombin generation can be made for plugs of plasma. We used a fluorogenic substrate for thrombin. When cleaved by thrombin, the fluorescence intensity of the substrate increases by ~ 10 -fold.⁹⁰ Thrombin is the final enzyme produced in the coagulation network, and it drives formation of the fibrin clot by cleaving fibrinogen. Fibrin clots form at low concentrations of thrombin (2–10 nM) while the majority of the thrombin (~ 1 μ M) is produced after the clot is fully formed.^{106,107} Thrombin favors cleaving fibrinogen compared to the substrate.^{107,108}

A single plug of plasma was followed as it traveled through the microchannel, and the fluorescence intensity was measured as a function of time (as shown for four plugs, each plug represented by one black dashed line, Figure 5b). Although the actual APTT of each individual plugs was different, the time taken for the relative fluorescence intensity to increase from 0 to 1 was the same. To determine the average APTT for many plugs, we correlated the detection of fibrin clots by bright-field microscopy to the detection of thrombin generation by fluorescence microscopy. Images were acquired at each time point by bright-field and fluorescence microscopy from the same experiment. Bright-field images were analyzed to determine the percentage of plugs clotted as a function of time. The APTT (~ 100 s) was determined to be the time at which 50% of the plugs contained fibrin clot (Figure 5b, red squares). This APTT correlated to a fluorescence intensity of $\sim 30\%$ of the maximum fluorescence signal (Figure 5b, blue circles).

Titration of Argatroban and Measurement of the APTT and Thrombin Generation

To determine the effect of the anticoagulant on the APTT, APTTs were measured while argatroban was titrated into samples of normal pooled plasma, donor's plasma, or donor's whole blood. Measuring the APTT of normal pooled plasma is a standard calibration procedure for coagulation instruments in central clinical laboratories. Therefore, we also obtained APTTs from normal pooled plasma. For on-chip titration, one of the two inlet streams of blood contained 3 $\mu\text{g}/\text{mL}$ argatroban. By varying the relative flow rates of these two blood streams, the concentration of argatroban within the plugs was varied.^{53,54} Experiments were conducted at 23 and 37 °C.

For experiments conducted at 23 °C, the effect of argatroban on thrombin generation for the donor's plasma samples agreed satisfactorily with the results from the normal pooled plasma (Figure 6a,b). The APTT ratio is the ratio of the APTT with argatroban in plasma to the baseline APTT without argatroban. For the donor's whole blood samples, the APTT ratio at 23 °C showed a dependence on the concentration of argatroban (Figure 6d). Generally, doses of argatroban between 0.2 and 2.0 $\mu\text{g}/\text{mL}$ are required to achieve an APTT ratio between 1.5 and 3.0. Using this on-chip APTT assay, an APTT ratio of 2.3 was reached for an argatroban dose of 0.5 $\mu\text{g}/\text{mL}$ and an APTT ratio of 2.8 for an argatroban dose of 1.0 $\mu\text{g}/\text{mL}$ at 23 °C (Figure 6d). For this donor, a nonlinear dependence of the APTT ratios on the concentration of argatroban was observed. This dependence was reproducible from experiments with plasma to experiments with whole blood (Figure 6b,c).

Two modifications from the protocol were required to conduct experiments at the physiological temperature of 37 °C. First, a more concentrated Teflon AF solution (2.5% w/v instead of 1% w/v for 23 °C measurements) was used to coat the microchannel to prevent the sticking of fibrin clots onto the microchannel walls. Fibrin clots were more likely to attach to the walls of the channel at higher temperatures. Second, a higher injection flow rate of the Alexin and blood sample was used to form larger plugs (the width-to-length ratio of the plug was $\sim 1:3$). While titrating argatroban in the same manner as the 23 °C experiments, APTTs were measured for normal pooled plasma (Figure 7a) and donor plasma (Figure 7b) at 37 °C. APTTs obtained at 37 °C were also ~ 2.5 times shorter than those at 23 °C. APTT ratios were similar at these two temperatures. Argatroban of 0.5 $\mu\text{g}/\text{mL}$ resulted in an APTT ratio of 2.3 at 23 °C (Figure 6d) and an APTT ratio of ~ 2.1 at 37 °C (Figure 7d). Argatroban of 1.0 $\mu\text{g}/\text{mL}$ resulted in an APTT ratio of 2.8 at 23 °C (Figure 6d) and an APTT ratio of 2.7 at 37 °C (Figure 7d). APTT values and APTT ratios measured by the on-chip assay at 37 °C were compared to results from a clinical laboratory at 37 °C. Pooled plasma samples were mixed with argatroban (0–1.5 $\mu\text{g}/\text{mL}$) and submitted to the Coagulation laboratory at the University of Chicago Hospital for APTT measurements. APTTs obtained from the Coagulation laboratory were consistently about half of what we obtained from the on-chip assay (Figure 7c). However, the corresponding APTT ratios from these two methods agreed closely with each other (Figure 7d).

CONCLUSION

Two key technical developments enabled the work presented in this paper. First, the use of a Teflon AF coating helped minimize sticking of fibrin clots on the walls of microchannels. Second, reliable addition of a reagent from an aqueous stream into plugs was achieved by injecting the reagent stream through a hydrophilic narrow glass capillary. This merging method would be important for performing multistep assays and reactions in plugs, especially when cross-contamination must be minimized and ratios of reagents must be varied. Whereas bright-field measurements were a more qualitative metric, fluorescence measurements were used for quantitative analysis of thrombin generation within plugs. Rather than using a fluorescence microscope, the detection of fibrin clots within plugs can be simplified by using an array of LEDs,³² and this detection method would be compatible with plug-based microfluidics. The

methods developed in this paper would be useful for other assays using blood, including the prothrombin time assay, the dose determination of heparin and other anticoagulant drugs in blood samples, and the detection of other analytes within the blood samples. Heparin is a widely used anticoagulant, and dose determination of heparin is frequently determined by point-of-care devices, which is especially essential during cardiac surgery.³² Using segmented flow of air and liquid, flow injection analysis was used to determine the levels of eight analytes within a sample of blood.⁴² These results were obtained and forwarded to the physician within 30 min. Rapidly performing multiple tests and dose determinations on a single blood sample using preloaded reagent cartridges¹⁰⁹ is an exciting opportunity that can be realized with this plug-based microfluidic system. In this paper, measurement of the APTT was simplified by using a computer-controlled stage to move the field of view over the microfluidic channel and using a program to automate the acquisition of images at each stage position.

Many types of single-use multichannel devices are already commercially available. These systems are easy to use as all the components necessary for mixing, addition of reagents, and detection of the fibrin clot are fully integrated into a single machine. These systems have had an important impact in critical surgery procedures where a rapid determination of the clotting time is necessary. One system has used multichannel devices to perform titration experiments to measure the heparin levels in blood and to measure the platelet-activated clotting test.³² To measure heparin levels, several channels in a single device contained varying levels of protamine, where protamine neutralized the anticoagulant properties of heparin. To measure the platelet-activated clotting test, each channel in the device contained increasing concentrations of platelet-activating factor. Using this system, each channel required ~800 μL of blood and so several milliliters of blood are needed to perform these titration assays. Using plug-based microfluidics, each plug contained ~40 nL of the blood sample. To determine the clotting time at each concentration of argatroban, the clotting time was measured for at least 140 plugs, where each plug can be considered to be an independent experiment. Analysis of the data was simplified by using an optical microscope with an automated stage. To obtain the APTT for four concentrations of argatroban, less than 24 μL of blood sample was needed. By using a preformed cartridge¹⁰⁹ containing various clotting agents and reagents, many different types of assays can be performed with a small amount of blood sample. This feature is particularly useful for blood samples that are only available in small quantities, such as samples from children and infants^{110,111} or small model organisms.^{112–115}

To establish the medical value of this rapid microfluidic titration assay, a clinical study would be required. Ideally, for each patient, one would use the microfluidic system to predict the correct dose of an anticoagulant drug, administer the drug, and then validate the prediction by retesting the clotting properties of the blood sample. In vitro, these microfluidic measurements do not take into account the pharmacokinetics of the drug. For example, these measurements would not be valid for the drug warfarin, which works by decreasing the production of clotting factors in the liver. In the case of argatroban, elimination of the drug varies from patient to patient further complicating matters. A procedure remains to be established for correlating the results of microfluidic titrations to the predicted dose for a patient. Such a study is outside the scope of this paper, which focused on developing microfluidic techniques and on characterization of this plug-based assay. Now that the microfluidic system is developed and validated, such a clinical study would be ethically more acceptable and more informative. The APTT ratios from the two methods (clinical lab versus the on-chip assay) agreed well with each other. However, the difference in the actual APTT values from these two methods was interesting. Variations are common among commercial coagulation instruments, where potential reasons include the differences in sample volume and sample manipulation and in material composition of the measuring devices.¹¹⁶ Using plug-based microfluidic devices provides opportunities to understand and explain these differences, by controlling the sample volume and the interfacial interaction between the blood sample and the wall of the devices.

Preliminary results (data not shown) indicated that slower initiation of clotting inside plugs may be due to more efficient mixing in plugs,⁴⁷ where mixing effects are commonly observed in autocatalytic systems;⁹⁸ smaller volume of plugs, where volume effects have been observed in nonlinear systems;¹¹⁷ and a cleaner interface⁵¹ between the plug and the surrounding fluorinated carrier fluid. A more detailed investigation of these effects will be important for understanding of the effects of miniaturization on clotting tests. We are especially interested in using these effects and methods to understand the complex reaction network of blood clotting.¹¹⁸

Acknowledgements

This work was supported by NIH (R01 EB001903) and performed in part in the MRSEC microfluidic facility funded by NSF. We thank Jeffrey Gist, Krzysztof Mikrut, and Charlot Webb from the Coagulation Lab at the University of Chicago Hospital for measurement of the APTT with the commercial STA Coagulation instrument. We thank Matthew Runyon and Christian Kastrup for invaluable suggestions and assistance. We thank Bethany Johnson-Kerner for preliminary results. We thank Dr. Jonathan Miller and Dr. Rocky Shiu-ki Hui for helpful discussions. We thank Liang Li for surface tension and viscosity measurements for the carrier fluid.

References

1. Beutler, E.; Lichtman, MA.; Coller, BS.; Kipps, TJ. *Williams Hematology*. 5th ed. McGraw-Hill; New York: 1995.
2. Warkentin TE. *Thromb Res* 2003;110:73–82. [PubMed: 12893020]
3. Warkentin TE. *Br J Haematol* 2003;121:535–555. [PubMed: 12752095]
4. Francis JL, Hursting MJ. *Blood Coagulation Fibrinolysis* 2005;16:251–257. [PubMed: 15870544]
5. Boldt J, Walz G, Triem J, Suttner S, Kumle B. *Intensive Care Med* 1998;24:1187–1193. [PubMed: 9876982]
6. Sia SK, Whitesides GM. *Electrophoresis* 2003;24:3563–3576. [PubMed: 14613181]
7. Beebe DJ, Mensing GA, Walker GM. *Annu Rev Biomed Eng* 2002;4:261–286. [PubMed: 12117759]
8. Auroux PA, Iossifidis D, Reyes DR, Manz A. *Anal Chem* 2002;74:2637–2652. [PubMed: 12090654]
9. McDonald JC, Whitesides GM. *Acc Chem Res* 2002;35:491–499. [PubMed: 12118988]
10. Ahn CH, Choi JW, Beaucage G, Nevin JH, Lee JB, Puntambekar A, Lee JY. *Proc IEEE* 2004;92:154–173.
11. Bange A, Halsall HB, Heineman WR. *Biosens Bioelectron* 2005;20:2488–2503. [PubMed: 15854821]
12. Toner M, Irimia D. *Annu Rev Biomed Eng* 2005;7:77–103. [PubMed: 16004567]
13. Hayashi K, Iwasaki Y, Kurita R, Sunagawa K, Niwa O. *Electrochem Commun* 2003;5:1037–1042.
14. Weigl BH, Kriebel J, Mayes KJ, Bui T, Yager P. *Mikrochim Acta* 1999;131:75–83.
15. Du Y, Yan JL, Zhou WZ, Yang XY, Wang EK. *Electrophoresis* 2004;25:3853–3859. [PubMed: 15565683]
16. Yuen PK, Kricka LJ, Fortina P, Panaro NJ, Sakazume T, Wilding P. *Genome Res* 2001;11:405–412. [PubMed: 11230164]
17. Shevkoplyas SS, Yoshida T, Munn LL, Bitensky MW. *Anal Chem* 2005;77:933–937. [PubMed: 15679363]
18. Furdul VI, Harrison DJ. *Lab Chip* 2004;4:614–618. [PubMed: 15570374]
19. Takagi J, Yamada M, Yasuda M, Seki M. *Lab Chip* 2005;5:778–784. [PubMed: 15970972]
20. Petersson F, Nilsson A, Jonsson H, Laurell T. *Anal Chem* 2005;77:1216–1221. [PubMed: 15732899]
21. Kamada H, Hattori K, Hayashi T, Suzuki K. *Thromb Res* 2004;114:195–203. [PubMed: 15342216]
22. Katak AS, Gale BK, Lvov Y, Jones SA. *Biomed Microdevices* 2003;5:207–215.
23. Crowley TA, Pizziconi V. *Lab Chip* 2005;5:922–929. [PubMed: 16100575]
24. Kikuchi Y. *Microvasc Res* 1995;50:288–300. [PubMed: 8538506]
25. Srivastava N, Davenport RD, Burns MA. *Anal Chem* 2005;77:383–392. [PubMed: 15649032]

26. Tsukada K, Sekizuka E, Oshio C, Minamitani H. *Microvasc Res* 2001;61:231–239. [PubMed: 11336534]
27. Price AK, Fischer DJ, Martin RS, Spence DM. *Anal Chem* 2004;76:4849–4855. [PubMed: 15307797]
28. Gifford SC, Frank MG, Derganc J, Gabel C, Austin RH, Yoshida T, Bitensky MW. *Biophys J* 2003;84:623–633. [PubMed: 12524315]
29. Shelby JP, White J, Ganesan K, Rathod PK, Chiu DT. *Proc Natl Acad Sci USA* 2003;100:14618–14622. [PubMed: 14638939]
30. Murray ET, Fitzmaurice DA, McCahon D. *Br J Haematol* 2004;127:373–378. [PubMed: 15521913]
31. Tudos AJ, Besselink GAJ, Schasfoort RBM. *Lab Chip* 2001;1:83–95. [PubMed: 15100865]
32. Prisco D, Paniccia R. *Thromb J* 2003;1:1. [PubMed: 12904262]
33. Nutescu EA. *Semin Thromb Hemost* 2004;30:697–702. [PubMed: 15630676]
34. Bosch YPJ, Ganushchak YM, de Jong DS. *Perfusion-UK* 2006;21:27–31.
35. Dorfman DM, Goonan EM, Boutilier MK, Jarolim P, Tanasijevic M, Goldhaber SZ. *Vasc Med* 2005;10:23–27. [PubMed: 15920996]
36. Gardiner C, Williams K, Mackie IJ, Machin SJ, Cohen H. *Br J Haematol* 2005;128:242–247. [PubMed: 15638860]
37. Harrison P. *Blood Rev* 2005;19:111–123. [PubMed: 15603914]
38. Stewart KK. *Talanta* 1981;28:789–797.
39. Rocks B, Riley C. *Clin Chem* 1982;28:409–421. [PubMed: 7039868]
40. Stewart KK. *Anal Chem* 1983;55:A931.
41. Patton CJ, Crouch SR. *Anal Chim Acta* 1986;179:189–201.
42. Skeggs LT, Hochstrasser H. *Clin Chem* 1964;10:918. [PubMed: 14228271]
43. Skeggs LT. *Am J Clin Pathol* 1957;28:311–322. [PubMed: 13458160]
44. Tice JD, Song H, Lyon AD, Ismagilov RF. *Langmuir* 2003;19:9127–9133.
45. Song H, Tice JD, Ismagilov RF. *Angew Chem, Int Ed* 2003;42:768–772.
46. Shestopalov I, Tice JD, Ismagilov RF. *Lab Chip* 2004;4:316–321. [PubMed: 15269797]
47. Song H, Bringer MR, Tice JD, Gerds CJ, Ismagilov RF. *Appl Phys Lett* 2003;83:4664–4666. [PubMed: 17940580]
48. Bringer MR, Gerds CJ, Song H, Tice JD, Ismagilov RF. *Philos Trans R Soc London, Ser A* 2004;362:1087–1104.
49. Liao A, Kamik R, Majumdar A, Cate JHD. *Anal Chem* 2005;77:7618–7625. [PubMed: 16316169]
50. Gunther A, Jhunjhunwala M, Thalmann M, Schmidt MA, Jensen KF. *Langmuir* 2005;21:1547–1555. [PubMed: 15697306]
51. Roach LS, Song H, Ismagilov RF. *Anal Chem* 2005;77:785–796. [PubMed: 15679345]
52. Chen DL, Gerds CJ, Ismagilov RF. *J Am Chem Soc* 2005;127:9672–9673. [PubMed: 15998056]
53. Zheng B, Roach LS, Ismagilov RF. *J Am Chem Soc* 2003;125:11170–11171. [PubMed: 16220918]
54. Song H, Ismagilov RF. *J Am Chem Soc* 2003;125:14613–14619. [PubMed: 14624612]
55. Gerds CJ, Sharoyan DE, Ismagilov RF. *J Am Chem Soc* 2004;126:6327–6331. [PubMed: 15149230]
56. Anna SL, Bontoux N, Stone HA. *Appl Phys Lett* 2003;82:364–366.
57. Dreyfus R, Tabeling P, Willaime H. *Phys Rev Lett* 2003;90:Art. No. 144505
58. Garstecki P, Fuerstman MJ, Whitesides GM. *Phys Rev Lett* 2005;94:Art. No. 234502
59. Kobayashi I, Mukataka S, Nakajima M. *Langmuir* 2005;21:5722–5730. [PubMed: 15952815]
60. Okushima S, Nisisako T, Torii T, Higuchi T. *Langmuir* 2004;20:9905–9908. [PubMed: 15518471]
61. Tan YC, Fisher JS, Lee AI, Cristini V, Lee AP. *Lab Chip* 2004;4:292–298. [PubMed: 15269794]
62. Thorsen T, Roberts RW, Arnold FH, Quake SR. *Phys Rev Lett* 2001;86:4163–4166. [PubMed: 11328121]
63. Gordillo JM, Cheng ZD, Ganan-Calvo AM, Marquez M, Weitz DA. *Phys Fluids* 2004;16:2828–2834.
64. Umbanhowar PB, Prasad V, Weitz DA. *Langmuir* 2000;16:347–351.
65. Tice JD, Lyon AD, Ismagilov RF. *Anal Chim Acta* 2004;507:73–77. [PubMed: 17186061]
66. Curcio M, Roeraade J. *Anal Chem* 2003;75:1–7. [PubMed: 12530811]

67. Dorfman KD, Chabert M, Codarbox JH, Rousseau G, de Cremoux P, Viovy JL. *Anal Chem* 2005;77:3700–3704. [PubMed: 15924408]
68. Dittrich PS, Jahnz M, Schwille P. *Chembiochem* 2005;6:811–814. [PubMed: 15827950]
69. He MY, Edgar JS, Jeffries GDM, Lorenz RM, Shelby JP, Chiu DT. *Anal Chem* 2005;77:1539–1544. [PubMed: 15762555]
70. Noireaux V, Libchaber A. *Proc Natl Acad Sci USA* 2004;101:17669–17674. [PubMed: 15591347]
71. Grodrian A, Metze J, Henkel T, Martin K, Roth M, Kohler JM. *Biosens Bioelectron* 2004;19:1421–1428. [PubMed: 15093213]
72. Martin K, Henkel T, Baier V, Grodrian A, Schon T, Roth M, Kohler JM, Metze J. *Lab Chip* 2003;3:202–207. [PubMed: 15100775]
73. Yi GR, Jeon SJ, Thorsen T, Manoharan VN, Quake SR, Pine DJ, Yang SM. *Synth Met* 2003;139:803–806.
74. Yi GR, Manoharan VN, Klein S, Brzezinska KR, Pine DJ, Lange FF, Yang SM. *Adv Mater* 2002;14:1137–1140.
75. Kim JH, Choi WC, Kim HY, Kang Y, Park YK. *Powder Technol* 2005;153:166–175.
76. Jeong WJ, Kim JY, Choo J, Lee EK, Han CS, Beebe DJ, Seong GH, Lee SH. *Langmuir* 2005;21:3738–3741. [PubMed: 15835930]
77. Seo M, Nie ZH, Xu SQ, Lewis PC, Kumacheva E. *Langmuir* 2005;21:4773–4775. [PubMed: 15896006]
78. Gunther A, Khan SA, Thalmann M, Trachsel F, Jensen KF. *Lab Chip* 2004;4:278–286. [PubMed: 15269792]
79. Brito VO, Raimundo IM. *Anal Chim Acta* 1998;371:317–324.
80. Burns MA, Johnson BN, Brahmasandra SN, Handique K, Webster JR, Krishnan M, Sammarco TS, Man PM, Jones D, Heldsinger D, Mastrangelo CH, Burke DT. *Science* 1998;282:484–487. [PubMed: 9774277]
81. Cho SK, Moon HJ, Kim CJ. *J Microelectromech Syst* 2003;12:70–80.
82. Velev OD, Prevo BG, Bhatt KH. *Nature* 2003;426:515–516. [PubMed: 14654830]
83. Pollack MG, Fair RB, Shenderov AD. *Appl Phys Lett* 2000;77:1725–1726.
84. Pollack MG, Shenderov AD, Fair RB. *Lab Chip* 2002;2:96–101. [PubMed: 15100841]
85. Srinivasan V, Pamula VK, Fair RB. *Lab Chip* 2004;4:310–315. [PubMed: 15269796]
86. Srinivasan V, Pamula VK, Fair RB. *Anal Chim Acta* 2004;507:145–150.
87. Wheeler AR, Moon H, Kim CJ, Loo JA, Garrell RL. *Anal Chem* 2004;76:4833–4838. [PubMed: 15307795]
88. Wheeler AR, Moon H, Bird CA, Loo RRO, Kim CJ, Loo JA, Garrell RL. *Anal Chem* 2005;77:534–540. [PubMed: 15649050]
89. Millman JR, Bhatt KH, Prevo BG, Velev OD. *Nat Mater* 2005;4:98–102. [PubMed: 15608646]
90. Kawabata SI, Miura T, Morita T, Kato H, Fujikawa K, Iwanaga S, Takada K, Kimura T, Sakakibara S. *Eur J Biochem* 1988;172:17–25. [PubMed: 3278905]
91. Faber CG, Lodder J, Kessels F, Troost J. *Pathophysiol Haemostasis Thromb* 2003;33:52–58. [PubMed: 12853713]
92. Xia YN, Whitesides GM. *Angew Chem Int Ed* 1998;37:551–575.
93. McDonald JC, Duffy DC, Anderson JR, Chiu DT, Wu HK, Schueller OJA, Whitesides GM. *Electrophoresis* 2000;21:27–40. [PubMed: 10634468]
94. Choi WM, Park OO. *Microelectron Eng* 2003;70:131–136.
95. Mayer M, Kriebel JK, Tosteson MT, Whitesides GM. *Biophys J* 2003;85:2684–2695. [PubMed: 14507731]
96. Makohliso SA, Giovangrandi L, Leonard D, Mathieu HJ, Ilegems M, Aebischer P. *Biosens Bioelectron* 1998;13:1227–1235. [PubMed: 9871978]
97. Zheng B, Tice JD, Roach LS, Ismagilov RF. *Angew Chem, Int Ed* 2004;43:2508–2511.
98. Epstein IR. *Nature* 1995;374:321–327. [PubMed: 7885470]
99. Yen BKH, Gunther A, Schmidt MA, Jensen KF, Bawendi MG. *Angew Chem, Int Ed* 2005;44:5447–5451.

100. Gunther PM, Moller F, Henkel T, Kohler JM, Gross GA. *Chem Eng Technol* 2005;28:520–527.
101. Handique K, Burns MA. *J Micromech Microeng* 2001;11:548–554.
102. Doggett TA, Girdhar G, Lawshe A, Schmidtke DW, Laurenzi IJ, Diamond SL, Diacovo TG. *Biophys J* 2002;83:194–205. [PubMed: 12080112]
103. Mody NA, Lomakin O, Doggett TA, Diacovo TG, King MR. *Biophys J* 2005;88:1432–1443. [PubMed: 15533923]
104. Tandon P, Diamond SL. *Biophys J* 1997;73:2819–2835. [PubMed: 9370476]
105. Wolberg AS, Meng ZH, Monroe DM, Hoffman M. *J Trauma-Inj Infect Crit Care* 2004;56:1221–1228.
106. Brummel KE, Paradis SG, Butenas S, Mann KG. *Blood* 2002;100:148–152. [PubMed: 12070020]
107. Rand MD, Lock JB, vantVeer C, Gaffney DP, Mann KG. *Blood* 1996;88:3432–3445. [PubMed: 8896408]
108. Ramjee MK. *Anal Biochem* 2000;277:11–18. [PubMed: 10610684]
109. Zheng B, Ismagilov RF. *Angew Chem Int Ed* 2005;44:2520–2523.
110. Tan K, Booth D, Newell SJ, Dear PRF, Hughes C, Richards M. *Clin Lab Haematol* 2006;28:117–121. [PubMed: 16630216]
111. Nowatzke WL, Landt M, Smith C, Wilhite T, Canter C, Luchtman-Jones L. *J Pediatr Hematol Oncol* 2003;25:33–37. [PubMed: 12544771]
112. Jagadeeswaran, P.; Liu, YC.; Sheehan, JP. *Methods in Cell Biology*. Detrich, HW., III; Westerfield, M.; Zon, LE., editors. 59. Academic Press Inc.; San Diego: 1999. p. 337-357.
113. Jagadeeswaran P, Gregory M, Day K, Cykowski M, Thattaliyath B. *J Thromb Haemostasis* 2005;3:46–53. [PubMed: 15634265]
114. Hogan KA, Weiler H, Lord ST. *Thromb Haemostasis* 2002;87:563–574. [PubMed: 12008936]
115. Brodsky SV. *Exp Nephrol* 2002;10:299–306. [PubMed: 12381913]
116. van Oeveren W, Haan J, Lagerman P, Schoen T. *Artif Organs* 2002;26:506–511. [PubMed: 12072106]
117. Kondepudi DK, Asakura K. *Acc Chem Res* 2001;34:946–954. [PubMed: 11747412]
118. Runyon MK, Johnson-Kerner BL, Ismagilov RF. *Angew Chem, Int Ed* 2004;43:1531–1536.

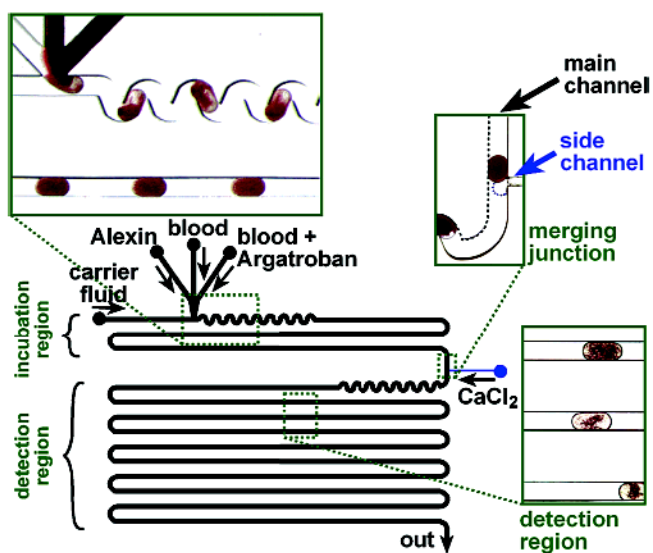


Figure 1. Schematic of a plug-based microfluidic device for determining the APTT and for titrating argatroban. Plugs containing Alexin (the APTT reagent) and blood (either plasma or whole blood) were formed in the plug-forming region, which were then transported to the incubation region (microphotograph, upper left). After flowing for 3 min, CaCl₂ solution was injected into each plug at the merging junction (microphotograph, upper right). The CaCl₂ droplet was traced with a dashed line in the microphotograph. In the detection region, clots formed within plugs were observed as a function of time (microphotograph, lower right).

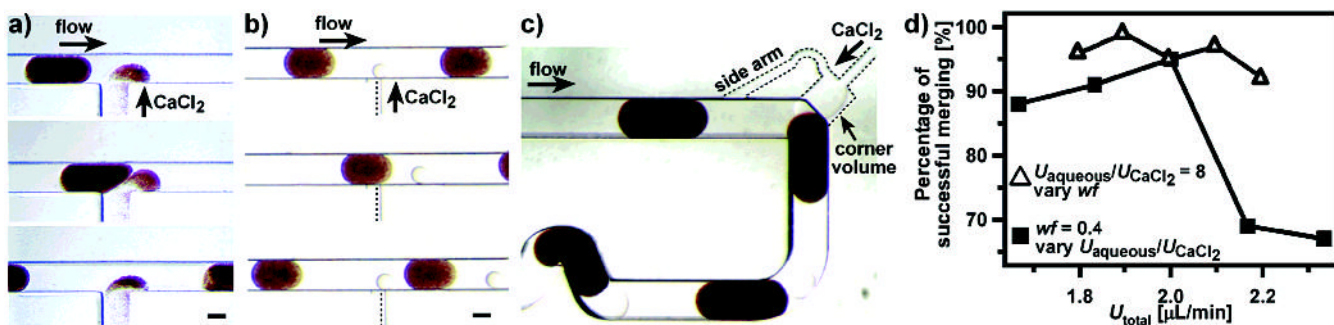


Figure 2.

Merging within a microfluidic device using a hydrophobic side channel. (a) When the side channel was hydrophobic (silanized PDMS), contamination occurred (for 5 out of 5 experiments) when the side channel was large (width of 200 μm and height of 250 μm). (b) However, merging did not occur (for 4 out of 4 experiments) when the side channel was too small (width and height of 20 μm). Another approach for merging was to form droplets of CaCl_2 at the same frequency as the passing plug. (c) At the junction, the carrier fluid between the passing plugs flows into the sidearm to break off a droplet from the CaCl_2 stream. (d) Consistent merging was obtained for $U_{\text{CaCl}_2}/U_{\text{aqueous}} = 0.125$ at various water fractions wf (\blacktriangle). At a constant wf = 0.4, high percentage of merging (95%) was measured only for $U_{\text{CaCl}_2}/U_{\text{aqueous}} = 0.125$ (\blacksquare). Each symbol represents measurements from 100 plugs. See text for definitions and details. All scale bars are for 100 μm .

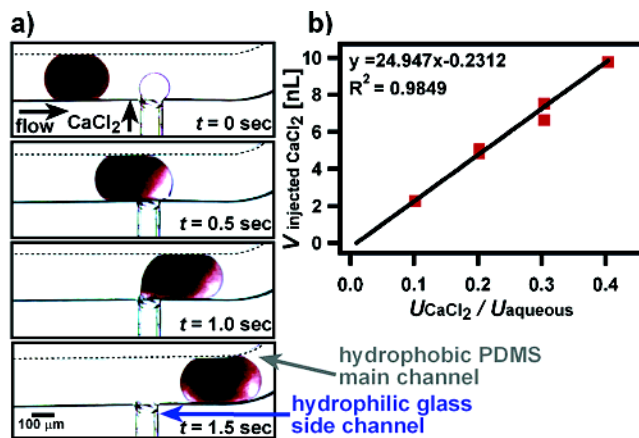


Figure 3.

(a) Consistent merging with a hydrophilic glass capillary inserted into the side channel. (b) The injection volume of CaCl_2 , $V_{\text{injected CaCl}_2}$ (nL), into the plug was controlled by flow rate ($\mu\text{L}/\text{min}$), where U_{CaCl_2} was the flow rate of the CaCl_2 stream and U_{aqueous} was the total aqueous flow rate for streams of Alexin and blood. In the graph, each symbol represents measurements for 10 plugs. At least two symbols are shown for each value of $U_{\text{CaCl}_2} / U_{\text{aqueous}}$, where some symbols coincide.

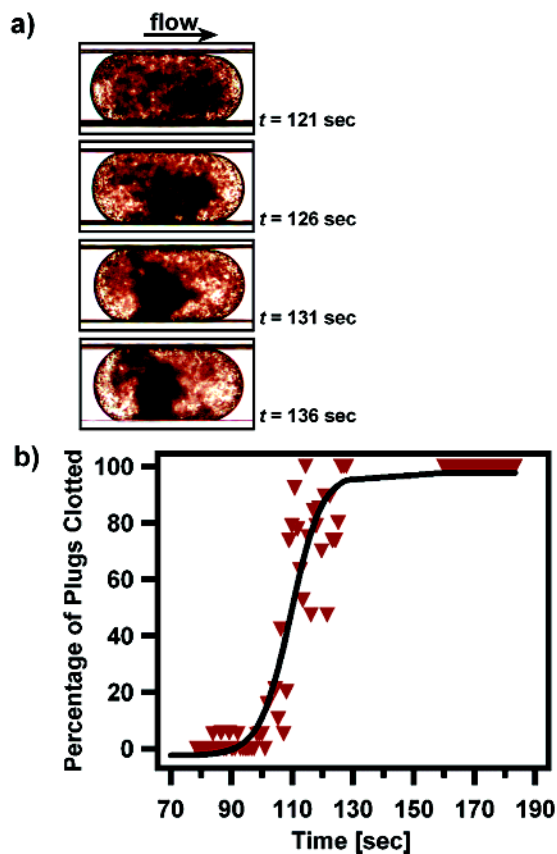


Figure 4.

Using bright-field microscopy to observe clots within plugs of whole blood. (a) A single plug of whole blood was followed as it traveled through the microchannel. Time t (s) was time for the plug traveled after merging with CaCl_2 . Whole blood within the plug was considered fully clotted when red blood cells were no longer moving inside the plug and a dense clot was observed within the back half of the plug (a, bottom image). (b) By analyzing images of plugs (as in a), the percentage of plugs that contained fibrin clots was determined for each time point in the detection region. A total of at least 20 plugs were used for each time point. Experiments were performed at 23 °C.

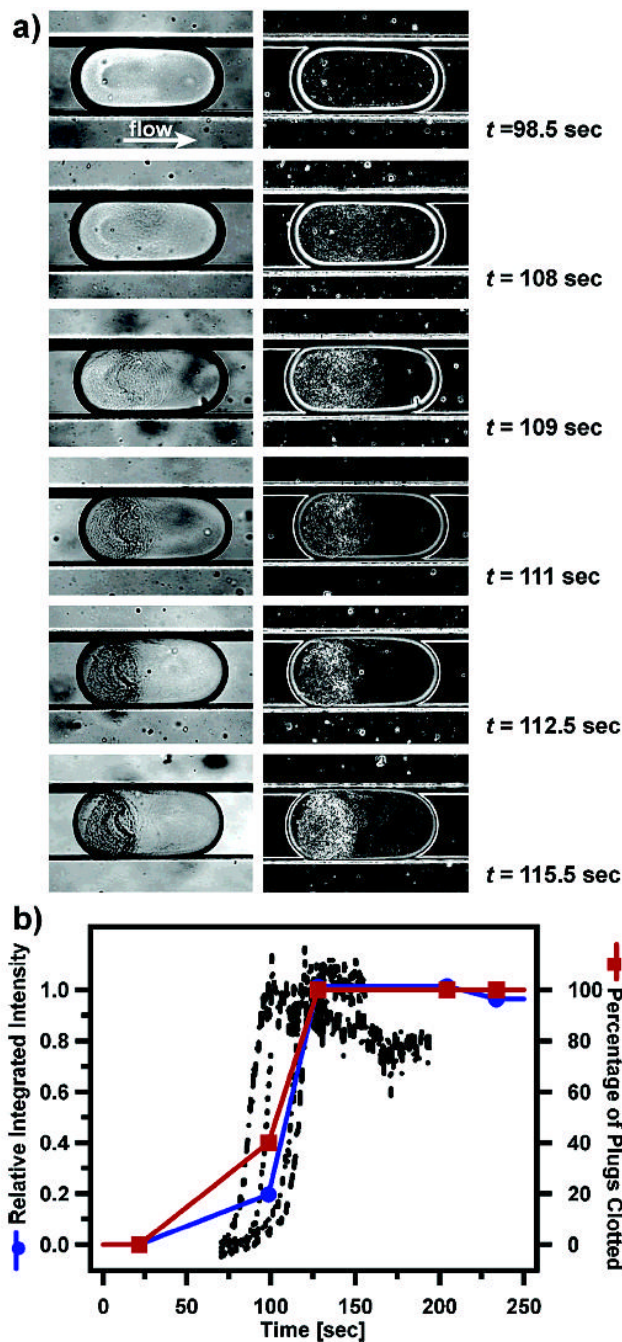


Figure 5. Using bright-field and fluorescence microscopy to observe the formation of fibrin clots within plugs of PRP. (a) A single plug of plasma was followed as it traveled through the microchannel (a, left panels). Bright-field images were processed with a digital Sobel filter to see clots more easily (a, right panels). Plasma was considered fully clotted when the fibrin clot condensed into the back half of the plug and sequential images of the plug looked the same (compare image at $t = 112.5$ s to image at $t = 115.5$ s). (b) Plugs were formed containing a fluorogenic substrate for thrombin in plasma. The fluorescence intensity of the substrate increases. In the graph, each black dashed line represents the fluorescence intensity arisen from an individual plug, where a single plug was followed as it traveled through the microchannel (total of 4 plugs

are shown). (•) Integrated intensities obtained from images collected with fluorescence microscopy were compared to (▪) the percentage of plugs clotted observed from images with bright-field microscopy. About 50% of the plugs were clotted when the fluorescence intensity was ~30% of the maximum fluorescence signal. Each symbol represents the measurement of at least 10 plugs at each time point in the detection region. Experiments were performed at 23 °C.

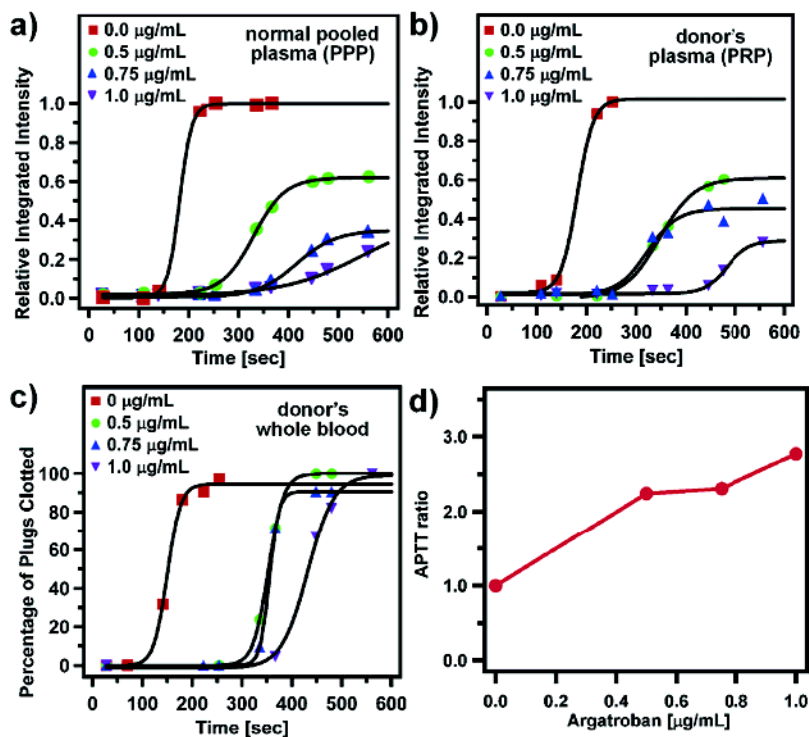


Figure 6. Measurement of thrombin generation and APTT at 23 °C while titrating argatroban into blood samples. (a, b) Detection of thrombin generation in plasma, (c) measurement of APTT in whole blood, and (d) the resulting APTT ratios for (c). The concentration of argatroban within the plugs was (\blacksquare) 0, (\bullet) 0.5, (\blacktriangle) 0.75, and (\blacktriangledown) 1.0 $\mu\text{g/mL}$. Each symbol represents the measurement of at least 20 plugs. (c) For whole blood samples, the APTT was the time at which the percentage of plugs clotted was 50%. (d) The APTT ratio was determined for the whole blood samples at each concentration of argatroban. The APTT ratio was the ratio of the APTT with argatroban to the baseline APTT without argatroban.

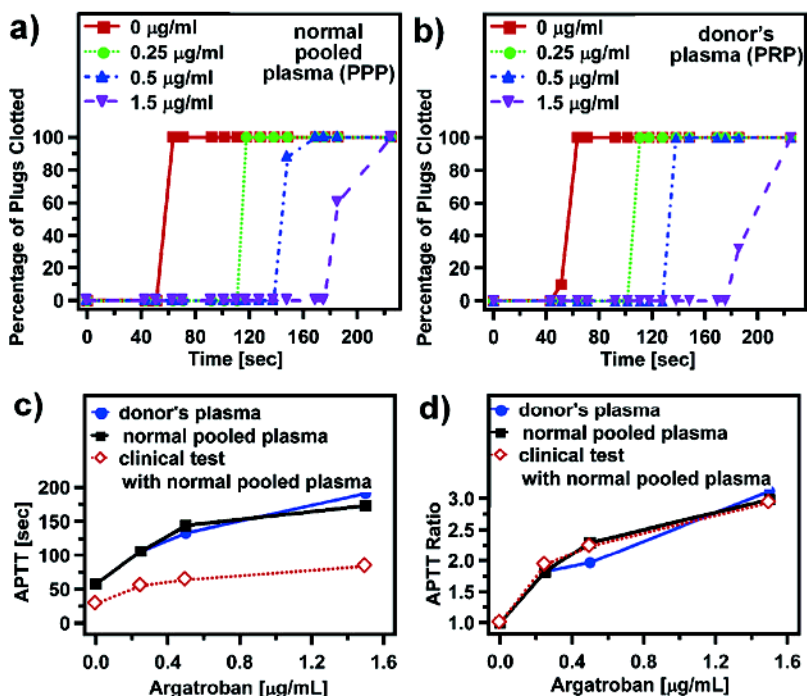


Figure 7. APTT measurements at 37 °C while titrating argatroban into (a) normal pooled plasma, and (b) donor plasma and corresponding values of the (c) APTT and (d) APTT ratios. For both plasma samples, the APTT was the time at which 50% of plugs contained fibrin clot. The concentration of argatroban within the plugs was (•) 0, (◐) 0.25, (▲) 0.5, and (▼) 1.5 μg/mL. Each symbol represents the measurement of at least 20 plugs. (c) The values of the (◐) clinical APTTs with normal pooled plasma were ~2 times lower than the APTTs measured with the plug-based microfluidic experiments with (•) normal pooled plasma and (◐) donor’s plasma. (d) The APTT ratios agreed well among the (◐) clinical APTTs with normal pooled plasma and the plug-based microfluidic experiments with (•) normal pooled plasma and (◐) donor’s plasma.